Benefits of Local Cooperation in Sectorized Cellular Networks Under a Complexity Constraint

Samet Gelincik, *Member, IEEE*, Michèle Wigger, *Senior Member, IEEE*, and Ligong Wang, *Member, IEEE*

***Abstract*— The paper presents upper and lower bounds on the per-sector degrees of freedom (DoF) of a sectorized hexagonal cellular model when neighboring base stations (BSs) can cooperate during at most Δ interaction rounds over rate-limited backhaul links. The lower bound is based on practically implementable beamforming and adapts the way BSs cooperate to the sectorization of the cells. It improves over the naive approach that ignores this sectorization in terms of the sum-rate, both at finite signal-to-noise ratio (SNR) and in the high-SNR limit. For moderate SNR, the new scheme improves also over an opportunistic cooperation strategy where each message is decoded based on the signals received at the three adjacent sectors with the best SNR. The upper bound is information-theoretic and holds for all possible coding schemes, including for example interference alignment with unlimited symbol extensions whose practical implementation currently seems out of reach. Lower and upper bounds show that the complexity constraint, imposed by limiting the number of interaction rounds Δ, indeed limits the largest achievable sum-rate and DoF. In particular, irrespective of the backhaul capacity μ, the per-sector DoF cannot exceed a threshold which depends on Δ.**

***Index Terms*— Cellular networks, cooperative multipoint (CoMP), degrees of freedom (DoF), genie-aided upper bound, hexagonal network, sector clustering.**

I. Introduction

THIS paper considers the uplink of a hexagonal cellular network with mobile users and base stations (BSs) that are equipped with multiple directional antennas, which allow them to create intracell sectors whose communications do not interfere. Inspired by current standards, each cell is divided into three sectors, and each BS has the same number M of antennas pointing at any of the cell's sectors. This model has received significant attention, e.g., in [2]–[4]. Here we follow the works in [5], [6], which entirely neglect interference between sectors in the same cell. In real systems this will not be the case, but since the interference is expected to be close to noise level, we shall ignore it in the present work. Our focus in this work will be on the sum-capacity of the hexagonal sectorized network model in the high signal-to-noise ratio (SNR) regime and the *degrees of freedom (DoF) per sector*.

The DoF of any generic [7] non-cooperative interference network with M-antenna receivers and sufficiently many transmit antennas is $M/2$ [7], [8]. Achieving this DoF however requires interference alignment techniques that currently cannot be implemented in practical systems. For the sectorized hexagonal model, a per-sector DoF of $M/2$ can also be achieved with more practical coding techniques such as one-shot interference alignment if the BSs can cooperate over backhaul links [5] which allow them to successively cancel part of the interference. On the negative side, the successive interference cancellation scheme proposed in [5] introduces arbitrarily long decoding delays, thus limiting its practical implementations. To avoid such long delays, in this paper we constrain the number of interaction rounds between BSs.

Yet another architecture that achieves DoF $M/2$ over any generic interference network is cloud radio-access networks (C-RANs) where all BSs are connected to a central processor over rate-limited fronthaul links [9]–[18]. In the downlink of a C-RAN, the central processor distributes the various messages or precoded signals over the fronthaul links to the different BSs. In the uplink, the central processor decodes all messages based on the compressed or (partially) decoded messages that it receives from the BSs. Achievability of DoF $M/2$ for the downlink C-RAN sectorized hexagonal model was proved in [6] with only moderate fronthaul capacities and using simple zero-forcing schemes and a smart assignment of the messages to the different BSs. Similar schemes can be designed for the uplink, for example based on the ideas in [19]. In C-RANs, fronthaul capacity is the only factor that limits cooperation as the central processor can convey any desired signal to the BSs. In particular, in this architecture there is no locality constraint in the sense that distributing correlated information to adjacent transmitting BSs is as resource-costly as distributing it over far away BSs. Such a model is tailored to the mentioned C-RAN architecture with a central processor directly connected to all the BSs. In this paper we are interested in a different scenario that is modelled by an interference network with cooperation links between neighbouring transmitters or receivers.

Manuscript received April 16, 2020; revised October 11, 2020 and January 7, 2021; accepted January 18, 2021. Date of publication February 1, 2021; date of current version June 10, 2021. The work of Michèle Wigger was supported in part by Huawei Inc. under Grant YB2015120036. This article was presented in part at the 15th International Symposium on Wireless Communication Systems, Lisbon, Portugal, August 28–31, 2018. The associate editor coordinating the review of this article and approving it for publication was K. Huang. *(Corresponding author: Michèle Wigger.)*

Samet Gelincik was with the LTCI, Communications and Electronics Department, Télécom Paris, 91120 Palaiseau, France. He is now with IETR, INSA de Rennes, 35708 Rennes, France and also with the Institut National de Sciences Appliquées (INSA) de Rennes, 35708 Rennes, France.

Michèle Wigger is with the LTCI, Communications and Electronics Department, Télécom Paris, 91120 Palaiseau, France (e-mail: michele.wigger@telecom-paristech.fr).

Ligong Wang is with ETIS Laboratory, UMR 8051, CY Cergy Paris Université, ENSEA, CNRS, 95000 Cergy-Pontoise, France.

Color versions of one or more figures in this article are available at https://doi.org/10.1109/TWC.2021.3054337.

Digital Object Identifier 10.1109/TWC.2021.3054337

Networks with transmitter or receiver cooperation have first been considered in [20], and subsequently in many other works such as [21]–[32]. In the context of cellular systems, cooperation has mostly been used to create diversity by relaying signals over alternate communication paths [21], [22], to enable coordinated scheduling and power allocation at the BSs [33], or to mitigate interference through *cooperative multipoint (CoMP)* transmission or reception, which is also known as *distributed or network multi-input multi-output (MIMO)* [28], [30], [31], [33]–[39]. In particular, in CoMP transmission, subsets of mobile users exchange (parts) of their messages and then jointly design their transmit signals based on this subset of messages, see e.g., [34]–[37]. In CoMP reception, subsets of receivers quantize and share their received signals over the cooperation links to a dedicated receiver that jointly decodes all the signals based on the obtained quantization outputs, see e.g., [28], [30], [31], [38], [39]. This latter mechanism is also known as clustered decoding [40] because clusters of messages are decoded jointly. Clustered decoding is also closely related to multi-access decoding [41] where *all* the messages are jointly decoded based on all receive signals. This fully-cooperative model can be considered as an extreme case of the C-RAN model with fronthaul links of unlimited rates. The performance of cellular networks with multi-access decoding has been studied in [4], [42]–[44].

In this work, we consider cooperation between receiving BSs and propose a new coding scheme based on the idea of CoMP reception with clustered decoding. The main contribution of our scheme is the specific way we build the clusters. One could be tempted to deactivate entire cells. We find a way to decompose the network into separate clusters by only deactivating the users in single sectors of certain cells but not the entire cells. Hereby we satisfy a given complexity constraint on the backhaul cooperation that restricts the number of interaction rounds, and as such the size of the clusters. The imposed complexity constraint is not active for various small networks, where few interaction rounds suffice, see e.g., [20], [23]–[25]. However, for large networks it has been shown that it can be beneficial if the number of interaction rounds grows with the number of users [29].

The main interest of this paper is to understand the maximum sum-rate and DoF that are achievable on the uplink of a sectorized hexagonal model when the backhaul cooperation between BSs is limited in capacity and in the number of interaction rounds. We provide upper and lower bounds on the maximum DoF and a lower bound on the maximum sum-rate. Our new lower bounds are based on the coding scheme described above and show that DoF $M/2$ is achievable in the sectorized hexagonal cellular model without interference alignment and with only two BS-interaction rounds and a backhaul DoF of $M/6$. Notice that a naive approach that builds the clusters by deactivating entire cells would need $M/3$ backhaul DoF to achieve $M/2$ DoF in the transmission from the mobile users to the BSs. Generally, our new clustering approach improves over this naive approach in all SNR ranges. At moderate and high SNRs our two-round cooperative scheme also improves over the practical scheme where each message is decoded based on the three neighbouring sectors that have strongest channel gains.

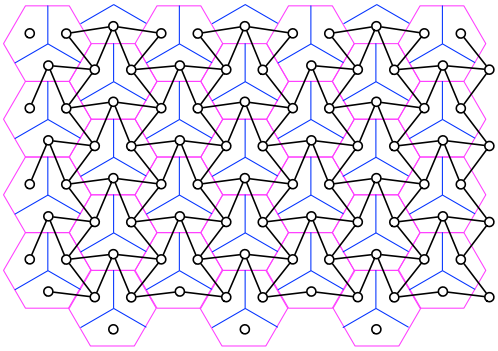

Fig. 1. Sectorized cellular model. Purple hexagonal regions depict the various cells and the blue lines divide them into sectors. Each node (small circle) depicts a sector with K mobile users that are each equipped with L transmit antennas. Each cell is associated to a BS, which for each of the three sectors has a set of M receive antennas directed to that sector.

The presented upper bound on the maximum DoF is information-theoretic and allows for any coding scheme. In particular, it includes other cooperation strategies beyond clustered decoding and interference alignment with unlimited symbol extensions, which is currently not implementable in practice. Since such interference alignment is commonly known to improve over the simple beamforming techniques applied in our coding scheme, the proposed upper and lower bounds do not match in general. Nevertheless, the information-theoretic upper bound still provides a benchmark for our practical scheme. The information-theoretic upper bound further shows that, irrespectively of the capacities of the backhaul links, the DoF is bounded away from M when the maximum number of cooperation rounds Δ is finite.

To summarize, our main contributions in this paper are:

- We propose a new BS-cooperation scheme for the uplink of a sectorized hexagonal network with M antennas in each sector.
  - Our scheme is based on simple CoMP reception and no interference alignment.
  - It achieves DoF $M/2$ with only two interaction rounds between adjacent receivers. (For comparison, notice that the scheme in [5] required an unlimited number of rounds.)
  - At moderate SNR our scheme improves over previous schemes used in practice.
- We prove a new information-theoretic upper bound on the DoF of the uplink of a sectorized hexagonal network with M antennas in each sector under a complexity constraint on the number of allowed interaction rounds Δ. The bound shows that for finite Δ the DoF is bounded away from M even under unlimited backhaul capacity. (This is obviously not the case for an unlimited number of interaction rounds, where DoF M is achievable with sufficiently large backhaul loads.)

II. Problem Definition

A. Network Model

Consider the uplink communication of a cellular network consisting of $N \gg 1$ hexagonal cells as depicted in Figure 1.

Each cell contains a BS equipped with $3M$ directional antennas, where a third of these antennas covers each of the three sectors of the cell. Usage of directional antennas, where side lobe radiation patterns are negligible, implies that interference between the three sectors in the same cell is negligible. This leads to the interference graph in Figure 1, where each sector is depicted by a node (small circle), and interfering sectors in different cells are connected by solid black lines, whereas noninterfering sectors in the same cell are not connected. In each sector there are K mobile users, each equipped with L antennas. As is often the case in practical systems, we assume that

$$K \cdot L \geq M, \tag{1}$$

i.e., there are more transmit than receive antennas in each sector. The uplink communication is modeled by the following discrete-time input-output relation:

$$\mathbf{y}_{u,t} = \sum_{k=1}^{K} \mathbf{H}_{u,u}^{(k)} \mathbf{x}_{u,t}^{(k)} + \sum_{\substack{v:\ \text{sector } v \\ \text{interferes sector } u}} \sum_{k=1}^{K} \mathbf{H}_{u,v}^{(k)} \mathbf{x}_{v,t}^{(k)} + \mathbf{z}_{u,t}, \tag{2}$$

where

- $u \in \{1, \ldots, 3N\}$ denotes the index of a given cell-sector;
- $\mathbf{x}_{u,t}^{(k)}$ denotes the L-dimensional time-t signal sent by the k-th mobile user in sector u;
- $\mathbf{y}_{u,t}$ denotes the M-dimensional time-t signal received at the M BS receive antennas directing to sector u;
- $\mathbf{z}_{u,t}$ denotes the M-dimensional independent and identically distributed (i.i.d.) standard Gaussian noise vector corrupting the time-t signal at the receive antennas in sector u, which is independent of all other noise vectors; and
- $\mathbf{H}_{u',u}^{(k)}$ denotes an M-by-L matrix that models the channel from the k-th mobile user in sector u to the receive-antennas in sector u'.

Channel matrices are assumed to be constant during the entire transmission and known to all transmitters and receivers. We assume *generic* [7] channel coefficients, i.e., the entries of the channel matrices are drawn randomly and independently according to a continuous distribution. In our numerical simulations, we will assume more specifically that they are drawn according to independent Gaussian distributions.

B. Communication Model With Backhaul Cooperation

Fix a blocklength n, so the time index t takes value in $\{1, \ldots, n\}$. Consider the uplink communication over the cellular network described above where each of the K mobile users in sector $u \in \{1, \ldots, 3N\}$ wishes to send an independent message $W_u^{(k)}$ to the single BS in its cell. Here, $W_u^{(k)}$ is uniformly distributed over $\{1, \ldots, \lfloor 2^{nR_u^{(k)}} \rfloor\}$ with $R_u^{(k)}$ denoting its rate of transmission. Communication takes place in two phases. In the first phase, the k-th mobile user in sector u applies an encoding function $f_u^{(k)} \colon \{1, \ldots, \lfloor 2^{nR_u^{(k)}} \rfloor\} \to \mathbb{R}^{L \times n}$ to its message $W_u^{(k)}$ and sends the n resulting vectors

$$\mathbf{X}_u^{(k)} := (\mathbf{X}_{u,1}^{(k)}, \ldots, \mathbf{X}_{u,n}^{(k)}) = f_u^{(k)}(W_u^{(k)}) \tag{3}$$

as its inputs over the network. Each encoding function $f_u^{(k)}$ has to be chosen so that the input vectors satisfy an average input power constraint P:

$$\frac{1}{n} \sum_{t=1}^{n} \|\mathbf{X}_{u,t}^{(k)}\|^2 \leq P \quad \text{with probability 1.} \tag{4}$$

The subsequent second communication phase takes place after each receiving BS $j \in \{1, \ldots, N\}$ has observed all outputs at the antennas in each of the three sectors of the cell. The second phase takes place over the backhaul links connecting adjacent BSs, and it is assumed to be noise-free but rate-limited and can be interactive. However, to limit complexity and latency of the backhaul communications, we constrain the interaction to at most Δ rounds, for a given positive integer Δ.

For each $j \in \{1, \ldots, N\}$, let $\mathbb{Y}_j$ denote all the wireless signals observed at the $3M$ antennas of BS j:

$$\mathbb{Y}_j := \big\{(\mathbf{Y}_{u,1}, \ldots, \mathbf{Y}_{u,n})\colon \text{sector } u \text{ is in cell } j\big\}, \tag{5}$$

and let $\mathbb{V}_{\text{to } j}^{(d-1)}$ denote the $6 \cdot (d-1)$ cooperation messages BS j has received from its 6 neighboring BSs during the first $d-1$ cooperation rounds:

$$\mathbb{V}_{\text{to } j}^{(d-1)} := \big\{V_{i \to j}^{(d')}\colon \text{BS } i \text{ adjacent to BS } j \text{ and } d' = 1, \ldots, d-1\big\}. \tag{6}$$

In each cooperation round $d \in \{1, \ldots, \Delta\}$, each BS $j \in \{1, \ldots, N\}$ calculates the message $V_{j \to i}^{(d)}$ that it sends to a neighboring BS i as:

$$V_{j \to i}^{(d)} = \psi_{j \to i}^{(d)}\big(\mathbb{Y}_j, \mathbb{V}_{\text{to } j}^{(d-1)}\big), \tag{7}$$

for some cooperation functions $\big\{\psi_{j \to i}^{(d)}\big\}$ on appropriate domains. The cooperation functions have to be chosen such that for each pair of neighbouring BSs $i, j \in \{1, \ldots, N\}$, the total amount of information a BS j sends over the backhaul link to BS i does not exceed rate $\mu > 0$:

$$\frac{1}{n} \sum_{d=1}^{\Delta} \mathrm{H}\Big(V_{j \to i}^{(d)}\Big) \leq \mu, \tag{8}$$

where $\mathrm{H}(\cdot)$ denotes the entropy of a random variable [45]. In this paper, the backhaul load directly measures the number of bits sent over a given backhaul link connecting two neighbouring BSs. Moreover, we impose a "hard" *per-link* backhaul-load constraint. This differs significantly from the "soft" *average* backhaul-load constraint as in [46] where backhaul load refers to the number of messages available at each transmitter or the number of antennas accessible at each receiver, and where only the *average* load over all transmitters or receivers is limited.

Once the BS-cooperation phase is terminated, each BS $j \in \{1, \ldots, N\}$ proceeds to decode the $3K$ messages sent by the mobiles in the three sectors of its cell:

$$\mathbf{W}_j := \{W_u^{(k)}\colon \text{sector } u \text{ is in cell } j \text{ and } k = 1, \ldots, K\}. \tag{9}$$

To this end, it applies a decoding function h_j on corresponding domains to produce the message estimates

$$\hat{\mathbf{W}}_j := h_j\big(\mathbb{Y}_j, \mathbb{V}_{\text{to } j}^{(\Delta)}\big). \tag{10}$$

An error occurs in the communication unless for each cell $j \in \{1, \ldots, N\}$:

$$\hat{\mathbf{W}}_j = \mathbf{W}_j, \tag{11}$$

or equivalently, unless for each sector $u \in \{1, \ldots, 3N\}$ and user $k \in \{1, \ldots, K\}$ in this sector:

$$\hat{W}_u^{(k)} = W_u^{(k)}. \tag{12}$$

C. Sum-Capacity and Degrees of Freedom

A $3KN$-dimensional rate-tuple $(R_1^{(1)}, \ldots, R_{3N}^{(K)})$ is said to be achievable if, for every $\epsilon > 0$ and sufficiently large blocklength n, there exist encoding, cooperation, and decoding functions $\{f_u^{(k)}\}$, $\{\psi_{j,i}^{(d)}\}$, and $\{h_j\}$, such that

$$\mathbb{P}\left[\bigcup_{u=1}^{3N}\bigcup_{k=1}^{K}\{\hat{W}_u^{(k)} \neq W_u^{(k)}\}\right] \leq \epsilon. \tag{13}$$

The *capacity region* $\mathsf{C}(\mathsf{P}, \mu, \Delta)$ is defined as the closure of the set of all achievable rate-tuples, the *sum capacity* $\mathsf{C}_\Sigma(P, \mu, \Delta)$ is defined as

$$\mathsf{C}_\Sigma(P, \mu, \Delta) := \sup_{\substack{(R_1^{(1)}, \ldots, R_{3N}^{(K)}) \\ \in \mathsf{C}(P, \mu, \Delta)}} \sum_{u \in \{1, \ldots, 3N\}} \sum_{k=1}^{K} R_u^{(k)}, \tag{14}$$

and the *average per-sector capacity* $\bar{\mathsf{C}}(P, \mu, \Delta)$ is defined as

$$\bar{\mathsf{C}}(P, \mu, \Delta) := \frac{\mathsf{C}_\Sigma(P, \mu, \Delta)}{3N}. \tag{15}$$

In the high-SNR regime, the quantity of interest is the *per-sector degrees of freedom (DoF)*, which is defined as:

$$\mathsf{DoF}(\mu_{\text{DoF}}, \Delta) := \lim_{N \to \infty} \lim_{P \to \infty} \frac{\bar{\mathsf{C}}\left(P,\ \mu_{\text{DoF}} \cdot \frac{1}{2}\log(1+P),\ \Delta\right)}{\frac{1}{2}\log(1+P)}. \tag{16}$$

Notice that here the backhaul cooperation rate μ scales with the power constraint P:

$$\mu = \mu_{\text{DoF}} \cdot \frac{1}{2}\log(1+P). \tag{17}$$

Both the average per-sector sum capacity and the DoF of our system depend on the values of the channel matrices. In this manuscript we present bounds on the DoF that hold for all *generic channel matrices* [7], i.e., for a set of channel matrices that occur with probability 1 if the entries of the channel matrices are drawn independently of each other according to any continuous distribution. We also study lower bounds on the sum capacity at finite SNR when the channel gains are drawn according to Gaussian distributions.

III. Uplink Scheme With Cooperative BSs

In our scheme, some of the mobile users are deactivated, i.e., transmit no messages, and the other mobile users use multi-antenna Gaussian codebooks to send their own messages. (To attain fairness among users, different versions with different sets of deactivated mobile users can be time-shared or applied in different frequency bands.) Receiving BSs quantize their output signals and send the resulting quantization messages to specific BSs, which we call *master BSs*, where each master BS jointly decodes the subset of messages corresponding to the quantized output signals it receives. After this decoding step, the master BSs send back the decoded messages to the BSs to which the messages are actually intended. The main novelty in our work is a strategy to deactivate users so as to decompose the network into non-interfering clusters while keeping more users active than in the naive approach.

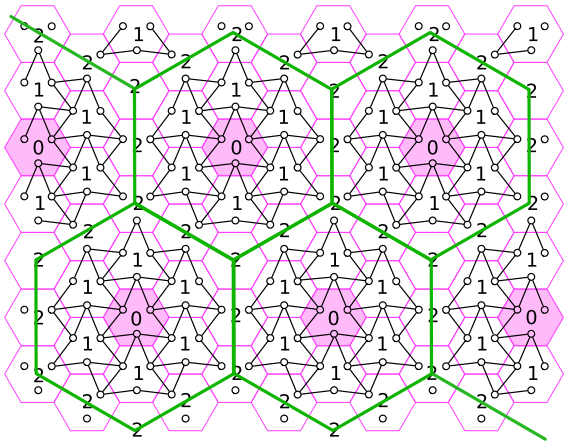

Fig. 2. Illustration of our uplink coding scheme with BS cooperation for parameter $\gamma = 2$. Magenta BSs decode all the messages sent by mobile users in the decoding regions defined by the green hexagons and then pass the decoded messages to their intended receiving BSs.

The single parameter of the scheme is the positive integer γ. As we will see, for a given parameter γ, cooperation takes place during 2γ rounds, and thus one is allowed to choose any

$$\gamma \in \left\{1, \ldots, \left\lfloor \frac{\Delta}{2} \right\rfloor\right\}. \tag{18}$$

For simplicity, we first consider the special case $\gamma = 2$. The general case is treated later.

A. Special Case $\gamma = 2$

Choose a set of BSs in such a way that they build a regular grid of corner points of equilateral triangles. The three corner points of any given triangle should be 4 cell hops apart, and there should be one cell that lies exactly 2 hops from each of them. Such a choice is depicted in Figure 2. The cells of the chosen BSs are coloured in magenta. We refer to cells that are adjacent to master cells as layer-1 cells, and the cells that are adjacent to layer-1 cells and are neither master cells nor layer-1 cells as layer-2 cells. Notice that we chose the master cells in such a way that every cell is either a master cell, a layer-1 cell or a layer-2 cell.

We then silence some of the sectors in the layer-2 cells, which we indicate in Figure 2 by omitting the nodes (small circles) in the center of these sectors. Silencing these transmitters eliminates some of the interference signals, and as such decomposes the network into non-interfering clusters (illustrated by green lines in Figure 2) around master BSs.

Encoding: Mobile users in the network that lie in sectors without nodes (small circles) in Figure 2 remain silent and

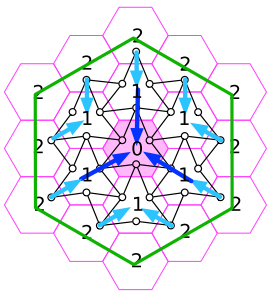

(a) Illustration of the first round cooperation messages from layer-2 BSs to layer-1 BSs (in light blue color) and from layer-1 BSs to master BSs (in dark blue color).

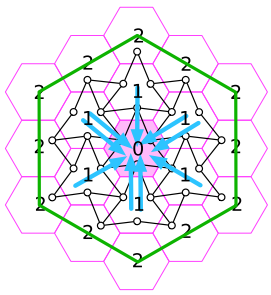

(b) Illustration of the second round cooperation messages from layer-1 BSs to master BSs. All these messages originally stem from the layer-2 BSs and are therefore depicted in light blue color.

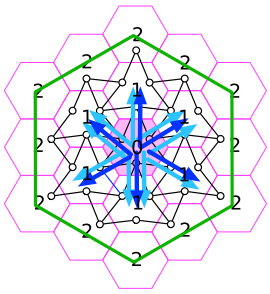

(c) Illustration of the third round cooperation messages from master BSs to layer-1 BSs. Messages that will be relayed to layer-2 BSs in round 4 are depicted in light blue color and messages that have layer-1 BSs as their final destination are in dark blue color.

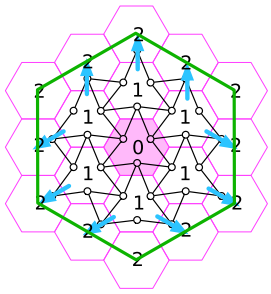

(d) Illustration of the fourth round cooperation messages from layer-1 BSs to layer-2 BSs.

Fig. 3. Illustration of the cooperation messages sent in the scheme when $\gamma = 2$.

do not transmit anything. All other mobile users transmit their messages using an independent Gaussian codebook of power P.

Cooperation Between BSs: Cooperation takes place over $2\gamma = 4$ rounds. The message flow is illustrated in Figure 3 and explained in the following.

- Round 1: Each layer-2 BS applies an independent rate-R_q (a parameter to be determined later) Gaussian vector quantizer to the M-dimensional receive signal of each of its sectors with active mobile users. It sends the quantization message obtained for a given sector to one of the adjacent layer-1 BSs that lie in the same cluster (in the same hexagonal region in Figure 2). Different routing options are possible for these messages, one possibility is shown in Figure 3a.
  Each layer-1 BS applies an independent rate-R_q Gaussian vector quantizer to each of its three M-dimensional receive signals, and it sends the 3 quantization messages to the adjacent master cell.
- Round 2: The layer-1 BSs forward the Round-1 messages they received from layer-2 BSs to their adjacent master BSs (see Figure 3b).
- Rounds 3 and 4: Each master BS uses the quantization messages received in Rounds 1 and 2 to reconstruct quantized versions of the 27 M-dimensional received signals observed in the sectors lying in the same cluster as the master BS itself. Using these 27 quantized M-dimensional signals and its own 3 M-dimensional receive signals, each master BS jointly decodes *all* the messages sent by the mobile users in the 30 active sectors of its cluster.
  In Rounds 3 and 4, messages decoded at the master BS but intended for layer-1 or layer-2 BSs are sent over the backhaul links to the intended BSs. Specifically, messages for layer-1 BSs are directly passed from the master BSs to their intended BSs in Round 3. Messages for layer-2 BSs are first passed to adjacent layer-1 BSs in Round 3, and then to the intended layer-2 BSs in Round 4. Different routing options exist for the cooperation messages intended for layer-2 BSs; one possibility is shown in Figures 3c and 3d.

Decoding: Each master BS declares the messages that it has produced during the decoding steps described at the beginning of cooperation-round 3. Each layer-1 BS declares the messages it has received during the cooperation round 3 and that were intended for it. Each layer-2 BS declares the messages that it has received during the cooperation round 4.

DoF Analysis: Choosing the quantization-rate as

$$R_q = M \cdot \frac{1}{2} \log(1 + P), \tag{19}$$

ensures that each received signal is essentially quantized at the noise level and allows the master BS to achieve the same DoF as if it directly had access to all the 30 receive signals in its cluster. Each cluster contains 30 active sectors with $30 \cdot M$ receive antennas and 30 KL transmit antennas, where recall that $KL \geq M$. It is easily verified that when the channel coefficients are chosen independently according to a continuous distribution, with probability 1 the rank of the channel matrix corresponding to the transmit and receive antennas in a single cluster equals 30 M. By symmetry, each of the 30 transmitted messages can thus have a rate corresponding to DoF M while the error probability is guaranteed to vanish. Notice now that for large networks ($N \to \infty$) a fraction of $\frac{5}{6}$ of the sectors are active, and thus the scheme achieves an average per-sector DoF of

$$\mathsf{DoF}_\gamma = M\frac{5}{6}, \qquad \gamma = 2. \tag{20}$$

Different instances of the proposed scheme, each time with a different set of master BSs and with different routing options, can be time-shared to balance the backhaul load. The total *per-link* backhaul load is then obtained by taking the average of the per-link backhaul loads over the various instances.

We analyze the total backhaul DoF in a given cluster. In Round 1, layer-2 BSs send 9 quantization messages in total, each of M DoF, to layer-1 BSs, and layer-1 BSs send in total 18 quantization messages, each of M DoF, to the

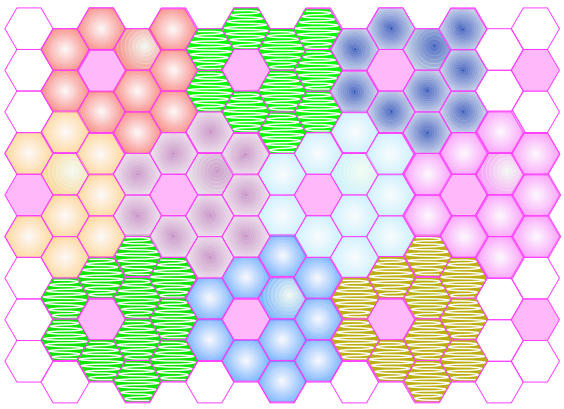

Fig. 4. Illustration of the proposed cell partitioning. The subsets of 11 cells associated to different master cells are shown in different colors and different shadings. (Master cells are in pink color).

adjacent master BS. In Round 2, layer-1 BSs send in total 9 quantization messages, each of M DoF, to the adjacent master BS. In Round 3, the master BS sends the decoded messages pertaining to 27 sectors to the 6 adjacent layer-1 BSs. The messages of 9 sectors are then further forwarded to adjacent layer-2 BSs during Round 4. Since all messages are assumed to be of equal rate and the total DoF of all the decoded messages in a cluster is 30 M, the backhaul DoF of Round 3 is 27 M (the same as in Round 1) and the backhaul DoF of Round 4 is 9 M (the same as in Round 2). So in total cooperation messages of DoF $72M$ are sent in each cluster.

To calculate this average backhaul DoF, notice that each green hexagonal region is associated with a single master cell, and that for $N \gg 1$ a cell partitioning can be obtained by associating 11 neighboring cells to each of the master cells as illustrated in Figure 4. (Note that the green hexagonal regions in Figure 2 do not represent a valid cell partitioning because some cells are associated with multiple master cells.) Including the master cell, each subset of the cell partitioning thus consists of 12 cells. Notice further that each cell is surrounded by 6 neighbouring cells and has 6 outgoing backhaul links. The average backhaul DoF *per cooperation link* is obtained by dividing the total backhaul DoF occupied in a single hexagonal region, i.e., $72M$, by the total number of backhaul links associated to a single subset of the cell partitioning, i.e., $6 \cdot 12$:

$$\mu_{\text{DoF},\gamma} = \frac{72M}{6 \cdot 12} = M, \qquad \gamma = 2. \tag{21}$$

B. General Case $\gamma > 0$

Choose the master cells so that they form a regular pattern of equilateral triangles and the master cells corresponding to the three corner points of such a triangle are 2γ cell-hops apart, and there should be one cell that is γ hops apart from each of them. (Notice that all valid choices can be obtained from each other by translation.) For $\ell = 1, \ldots, \gamma$, we call *layer-ℓ* cells, the cells that are at distance ℓ from the closest master cell. The distance between two cells here is defined as the minimum number of cell-hops needed to get from one cell to the other.

Encoding: All mobile users in some sectors of the layer-γ cells are deactivated and do not transmit any message at all. All other mobile users are active, and send their messages using an independent Gaussian codebook of power P and same rate R. To describe the mobile users that are deactivated, consider the layer-γ cells that are adjacent to 3 layer-$(\gamma - 1)$ cells. These cells will be called the *corner cells*. For every second of these corner cells, *all the mobile users in all three sectors are deactivated*; for all other corner cells, all mobile users in all three sectors are kept active. More specifically, for any two corner cells that are closest to each other, for one of them all users are deactivated and for the other one all users are active. For all other layer-γ cells, all mobile users are deactivated in the single sector that is closest to a corner cell with only active users. So, among all the layer-γ cells surrounding a master cell, 3 have only active users, 3 have only deactivated users, and the remaining $6(\gamma-1)$ have two sectors with active users and one sector with deactivated users.

Cooperation Between BSs: Cooperation takes place over 2γ rounds.

- Rounds 1 to γ: Each BS that is not a master BS applies a rate-R_q (a parameter to be determined later) Gaussian vector quantizer to any of its M-dimensional receive signals that correspond to a sector with active mobile users. For $\ell = 1, \ldots, \gamma - 1$, each layer-$\ell$ BS sends its 3 quantization messages to the closest master BS, by means of multi-hop communication over ℓ rounds. Each layer-γ BS sends each of its produced quantization messages to the master BS that is *closest to the sector* of each of the quantized signals. This transmission is again multi-hop over γ rounds.
- Rounds $\gamma + 1, \ldots, 2\gamma$: Each master BS reconstructs the M-dimensional quantized signals corresponding to the quantization messages received in Rounds $1, \ldots, \gamma$. It then jointly decodes the messages sent by the mobile users in the sectors corresponding to these quantization messages as well as the messages sent by the mobile users in its own cell. Finally, during cooperation rounds $\gamma + 1, \ldots, 2\gamma$, it communicates each of the decoded messages using multi-hop communication to its intended BS.

Decoding: Each master BS directly declares the messages guessed for its own cell before cooperation round $\gamma + 1$. The other BSs declare the messages that the master BSs have guessed for their cells and which they have learned during cooperation rounds $\gamma + 1, \ldots, 2\gamma$.

IV. Achievable Rates and Bounds on the DoF

A. High-SNR DoF Results

Based on the scheme in the preceding section and a new information-theoretic converse (see Appendix B), we present lower and upper bounds on the DoF of the sectorized hexagonal network with generic [7] channel coefficients.

Define $\mu_{\text{DoF},0} = 0$ and $\text{DoF}_0 = \frac{M}{3}$, and for each $\gamma \in \{1, \ldots, \lfloor \frac{\Delta}{2} \rfloor\}$:

$$\mu_{\text{DoF},\gamma} := M \frac{2\gamma - 1}{3} \tag{22}$$

$$\text{DoF}_\gamma := M\Big(1 - \frac{1}{3\gamma}\Big). \tag{23}$$

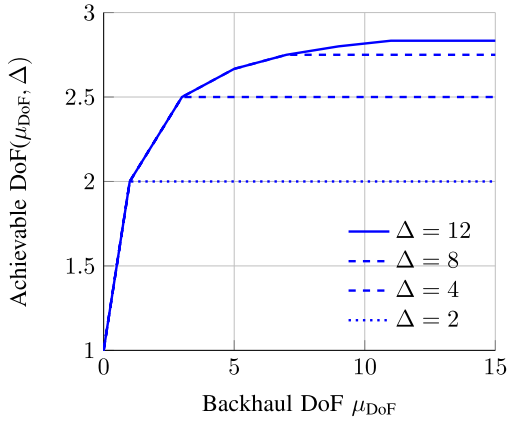

Fig. 5. Lower bound in Theorem 1 for different values of Δ and $M = 3$, as a function of μ_{DoF}.

Theorem 1 (Achievability): For generic channel coefficients, the DoF is lower bounded as

$$\begin{aligned}&\mathsf{DoF}\left(\mu_{\text{DoF}}, \Delta\right)\\ &\geq \text{upp conv hull}\Big\{\left(\mu_{\text{DoF},\gamma}, \text{DoF}_{\gamma}\right) : \gamma = 0, \ldots, \Big\lfloor \frac{\Delta}{2} \Big\rfloor\Big\}. \quad (24)\end{aligned}$$

Proof: The claim follows by time-sharing the scheme proposed in Section III for different values of γ. See Appendix A for details. ∎

Figure 5 illustrates this lower bound for different values of Δ. Even with only two conferencing rounds, a DoF of $M/2$ is achievable with our scheme using a backhaul DoF of only $\mu_{\text{DoF}} = 0.5$. Moreover, the DoF achieved by our scheme saturates at $\text{DoF}_{\lfloor \frac{\Delta}{2} \rfloor}$ irrespective of the available backhaul DoF. μ_{DoF}. As we will see from our converse result in Theorem 2 ahead, μ_{DoF} the ideal DoF of M cannot be approached even when $\mu \to \infty$.

Finally, the convex hull in Theorem 1 is simply given by the straight segments connecting the points $(\mu_{\text{DoF},0}, \text{DoF}_0)$, $(\mu_{\text{DoF},1}, \text{DoF}_1)$, $(\mu_{\text{DoF},2}, \text{DoF}_2)$, …, $(\mu_{\text{DoF},\lfloor \frac{\Delta}{2} \rfloor}, \text{DoF}_{\lfloor \frac{\Delta}{2} \rfloor})$, and the half-line to the right of $(\mu_{\text{DoF},\lfloor \frac{\Delta}{2} \rfloor}, \text{DoF}_{\lfloor \frac{\Delta}{2} \rfloor})$. This can be proved analytically using the fact that while DoF_{γ} is increasing in γ, the ratio $\frac{\text{DoF}_{\gamma}}{\mu_{\text{DoF},\gamma}}$ is decreasing in γ.

We compare the DoF in Theorem 1 to the DoF of the following *Naive Clustering Scheme*:

- *Naive Clustering Scheme* is a naive variation of our proposed scheme where for a given parameter γ, all layer-γ cells are deactivated. The admissible values for the parameter γ are thus $\gamma = 1, \ldots, \lfloor \frac{\Delta}{2} \rfloor + 1$. (Notice that the choice $\gamma = 1$ splits the networks into isolated cells and the scheme does not exploit the cooperation links at all.) Following similar steps as in the analysis of our new scheme in Appendix A, it can be shown that for any fixed $\gamma \in \{1, 2, \ldots, \lfloor \frac{\Delta}{2} \rfloor + 1\}$, the naive scheme achieves the backhaul-rate DoF pair:

$$\mu_{\text{naive},\gamma} := M\frac{(2\gamma - 1)(\gamma - 1)}{3} \quad (25)$$

$$\text{DoF}_{\text{naive},\gamma} := M\left(1 - \frac{3\gamma - 1}{3\gamma^2}\right). \quad (26)$$

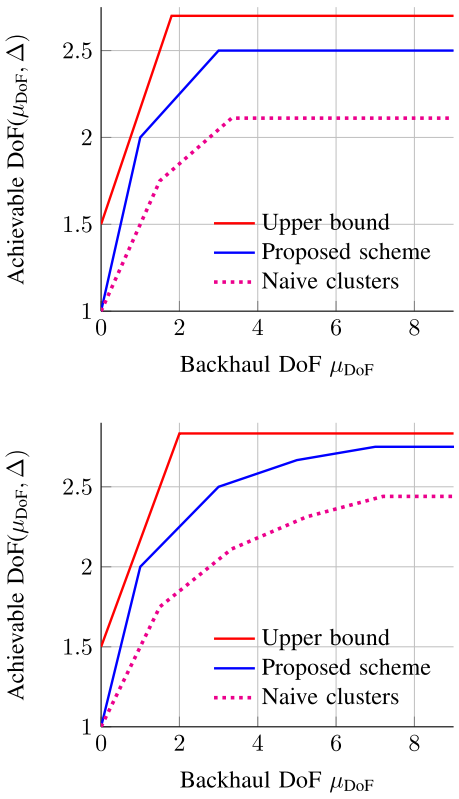

Fig. 6. Lower and upper bounds on the DoF as functions of μ_{DoF} for $M = 3$. The figure on the left is for $\Delta = 4$ and the figure on the right for $\Delta = 8$.

The DoF achieved by this naive scheme (Scheme 2) is thus equal to

$$\begin{aligned}\text{DoF}_{\text{naive}} = \text{upp conv hull}\Big\{&\left(\mu_{\text{naive},\gamma}, \text{DoF}_{\text{naive},\gamma}\right) :\\ &\gamma = 1, 2, \ldots, \Big\lfloor \frac{\Delta}{2} \Big\rfloor + 1\Big\}. \quad (27)\end{aligned}$$

Figure 6 compares the new lower bound in Theorem 1 with the lower bound (27). The figure also shows the information-theoretic upper bound stated below. Notice that the lower bounds on the DoF are based on practically implementable coding schemes. In particular, classical interference alignment is not used, even though it is known to achieve a DoF of $M/2$ over a generic network in the absence of BS cooperation. In contrast, the information-theoretic upper bound holds for any possible coding scheme, obviously including interference alignment. It is thus natural that there is a gap between the presented upper and lower bounds.

Theorem 2 (Converse): If $M = KL$, the DoF is upper bounded as

$$\mathsf{DoF}\left(\mu_{\text{DoF}}, \Delta\right) \leq \min\left\{\frac{M}{2} + \frac{2}{3}\mu_{\text{DoF}},\ M\left(1 - \frac{1}{2(\Delta + 1)}\right)\right\}. \quad (28)$$

Proof: See Appendix B. ∎

Interestingly, even when the backhaul prelog $\mu_{\text{DoF}} \to \infty$, the maximum $\mathsf{DoF}\left(\mu_{\text{DoF}}, \Delta\right)$ is bounded by $M\left(1 - \frac{1}{2(\Delta+1)}\right)$, and thus the complexity constraint Δ is stringent. In fact, if both $\Delta \to \infty$ and $\mu_{\text{DoF}} \to \infty$, then trivially a DoF of

M is achievable, because all BSs can fully cooperate and the setup reduces to a multi-access scenario.

We now consider the largest additive gap between the upper and lower bounds of Theorems 1 and 2. Using simple algebraic arguments, it can be shown that, for $\Delta = 1, 2$ the largest additive gap is attained at $\mu = 0$; for $\Delta = 3, \dots$ it is attained at $\mu_{\text{DoF}} = \frac{3\Delta}{4(\Delta+1)}$, which is the backhaul DoF where the two terms in the minimization (28) coincide and the upper bound becomes constant. As a consequence:

$$\text{largest additive gap} = \begin{cases} M/6, & \Delta = 1, 2 \\ M/3 - M/(2(\Delta+1)), & \Delta = 3 \\ M/12 - M\frac{3\Delta+8}{16(\Delta+1)}, & \Delta \geq 4. \end{cases} \tag{29}$$

To determine the largest multiplicative gap, we notice that at μ_{DoF} the gap is $3M/2$ and that for all values $\mu_{\text{DoF}} \geq \mu_{\text{DoF},1}$ the gap is less than $3M/2$ because the upper bound is less than M and the lower bound is at least $2M/3$. A simple inspection reveals that also in the regime $\mu_{\text{DoF}} \leq \mu_{\text{DoF},1}$ the multiplicative gap cannot be larger than $3M/2$. Therefore:

$$\text{largest multiplicative gap} = M\frac{3}{2}. \tag{30}$$

B. Finite SNR Results

To describe the rates achieved by our scheme at finite SNR, we denote by J the number of clusters in the system and for each $j = 1, 2, \dots, J$ by $\mathsf{H}_{\gamma,j}$ the submatrix of H including all the sectors that belong to a given cluster j. Notice that for most clusters, $\mathsf{H}_{\gamma,j}$ is of dimension $3\gamma(3\gamma-1) \times 3\gamma(3\gamma-1)$; only for clusters at the edge of the network can it be smaller. For simplicity of exposition, we will only consider the full clusters, which would be dominant in large networks.

Proposition 3: For any parameter $\gamma \in \{0, 1, \dots, \lfloor \Delta/2 \rfloor + 1\}$, the scheme in Section III achieves an average per-user rate $R_{\text{per-user}} = \frac{1}{NK}(R_1^{(1)} + \cdots R_{3N}^{(K)})$ equal to

$$R_{\text{per-user}} = \frac{1}{J}\sum_{j=1}^{J} \frac{1}{18\gamma^2} \cdot \log \frac{|P\mathsf{H}_{\gamma,j}\mathsf{H}_{\gamma,j}^{\mathsf{T}} + \mathsf{I} + \Sigma_{q,\gamma}|}{|\mathsf{I} + \Sigma_{q,\gamma}|}, \tag{31}$$

where I denotes the identity matrix and $\Sigma_{q,\gamma}$ a diagonal matrix with diagonal entry 0 if the entry corresponds to the sector of the master cell and entry

$$\sigma_{q,u}^2 = \frac{P\|\mathbf{h}_u\|^2 + 1}{2^{\frac{6}{2\gamma-1}\mu} - 1}, \tag{32}$$

if the diagonal entry corresponds to any other given sector u of cluster j.

We numerically compare this rate to the rates of the naive clustering scheme described in the previous section and to the following two additional schemes:

- *Wind-spinner clusters* is a variation of our proposed scheme, where no users are silenced and interference from other clusters is treated as noise. The previously silenced users now also apply power-P Gaussian codebooks and their messages are decoded by the master cells of their clusters as explained before. Notice that the previously silenced users lie on the borders of different clusters, and one can therefore freely choose with which cluster to associate them. We here consider the regular "wind-spinner clusters" assignment described in our patent [47] and depicted in Figure 7, where each cluster is assigned the same number of "previously-deactivated" users. The comparison with our proposed scheme will suggest whether one should deactivate users at a certain SNR or not.
- *Opportunistic 3-BS clustering* is inspired by current practical systems. The decoding depends on the realization of the channel coefficients. With the help of its neighbors, each BS identifies for each user in its cell the 3 adjacent sectors that give the best *joint* decoding performance for the corresponding message. It then collects the (quantized versions of) these $3M$ output signals, and based on them decodes the desired messages. Notice that this scheme only involves one collaboration step and hence can be implemented for any positive cooperation complexity $\Delta \geq 1$.

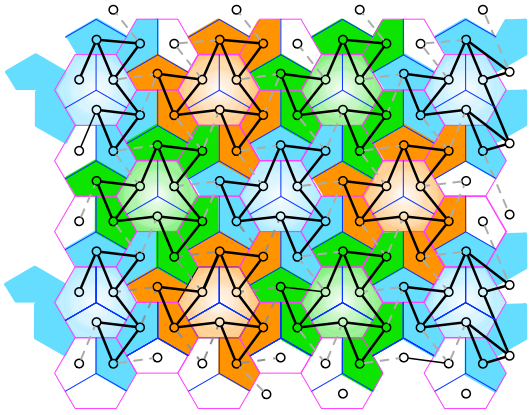

Fig. 7. Wind-spinner clustering as proposed in [47]. Different clusters are shown in different colors, master BSs are slightly shaded, and dashed lines depict interference between clusters.

Notice that these two additional schemes are not interesting in the high-SNR regime, because the processed signals are interfered by the signals from neighboring clusters. More specifically, the wind-spinner clustering approach cannot get a DoF larger than the scheme proposed in this paper, because the signals of the additionally activated cells all suffer from out-of-cluster interference. (The wind-spinner clustering scheme moreover requires higher backhaul DoF than our new scheme because more signals are quantized and sent to the master cell.) Even worse, the practical opportunistic BS-selection scheme typically does not achieve any positive DoF, because all signals are interfered from other signals sent from mobiles in other cells.

In our numerical comparison, we let the number of cells $N \to \infty$ to eliminate edge effects and average the rate over 5000 realizations of the channel matrices, where for each realization all channel gains are drawn independently of each other according to a Gaussian distribution. The direct channel gains of intra-sector links are drawn with variance 1 and the cross channel gains of inter-sector links are drawn with variance α, where α models the path attenuation. The backhaul capacity

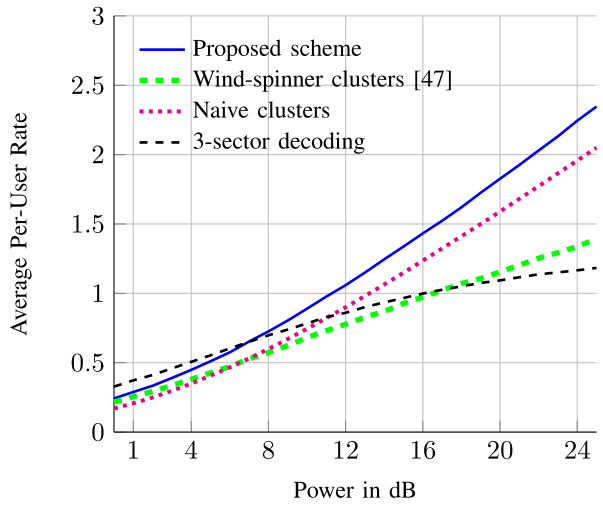

(a) Parameters $\alpha = 0.16$, $\mu_{\text{DoF}} = 0.5$, and $\Delta = 4$.

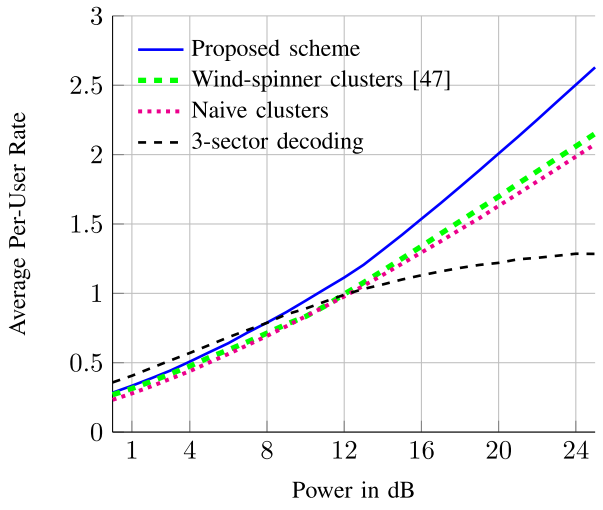

(b) Parameters $\alpha = 0.16$, $\mu_{\text{DoF}} = 1$, and $\Delta = 4$.

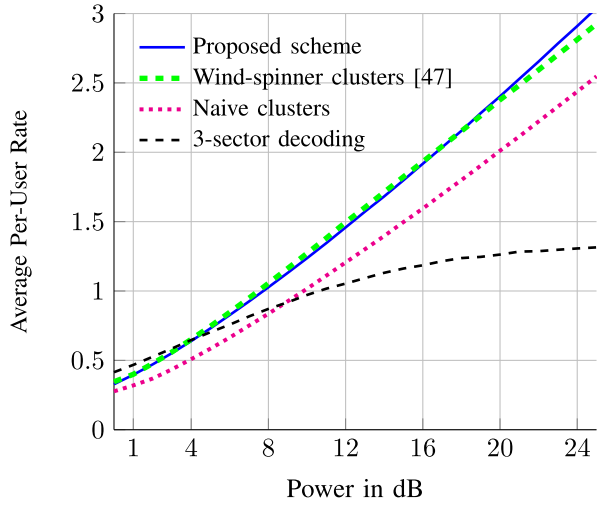

(c) Parameters $\alpha = 0.16$, $\mu_{\text{DoF}} = 2.5$, and $\Delta = 4$.

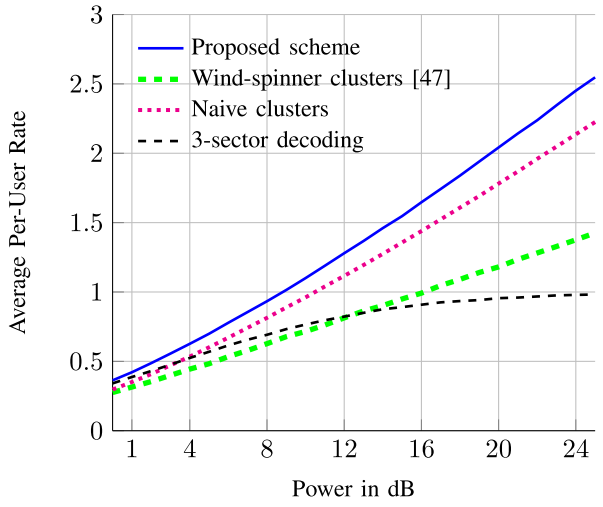

(d) Parameters $\alpha = 0.5$, $\mu_{\text{DoF}} = 1$, and $\Delta = 2$.

Fig. 8. Comparison of the rates achieved by the different schemes in the finite SNR regime.

is assumed to grow with power P as $\mu = \mu_{\text{DoF}} \cdot \frac{1}{2}\log(1+P)$, for a given backhaul DoF $\mu_{\text{DoF}} > 0$. Figure 8 shows the average rates of the different schemes as a function of the power P in dB for different choices of the path loss factor $\alpha \in \{0.16, 0.5\}$, the backhaul DoF $\mu_{\text{DoF}} \in \{0.5, 1, 2.5\}$, and the maximum allowed cooperation complexity $\Delta \in \{2, 4\}$. When $\Delta = 4$, for the scheme proposed in this paper and the wind-spinner cluster scheme in [47] the choices $\gamma = 1$ or $\gamma = 2$ are allowed. Notice that for a given quantization rate, it is always beneficial to choose γ as large as possible because it increases the benefit of cooperation. However, the larger γ, the more backhaul capacity is required. For a fixed backhaul capacity it can thus be beneficial to choose a smaller γ which allows to increase the quantization rate and thus the quality of the master BS's observations. Our numerical results reveal that for $\mu_{\text{DoF}} = 0.5$ and $\alpha = 0.16$ in both schemes it is optimal to choose parameter $\gamma = 1$ at all considered power levels. For a larger backhaul DoF, e.g., $\mu_{\text{DoF}} = 1$, in the newly proposed scheme the choice $\gamma = 1$ is optimal for powers below 13 dB and in the wind-spinner scheme of [47] it is optimal for powers below 10 dB. For larger powers the choice $\gamma = 2$ performs better. For the naive scheme that silences entire cells, parameters $\gamma = 1, 2, 3$ are possible when $\Delta = 4$. When $\alpha = 0.16$ for both $\mu_{\text{DoF}} = 0.5$ and $\mu_{\text{DoF}} = 1$, it is optimal to choose parameter $\gamma = 2$ at all power levels. For $\alpha = 0.16$ and $\mu_{\text{DoF}} = 2.5$, large quantization rates are available for all choices of γ, and as a consequence this parameter should be chosen as large as possible in all schemes and at almost all power levels (except for $P = 0$ or $P = 1$ dB). Similar observations hold also under a strong interference where $\alpha = 0.5$.

Comparing Figures 8a–8c, we observe that when $\alpha = 0.16$ and $\Delta = 4$, the opportunistic BS-selection scheme outperforms the others at small power levels. At higher power levels however the performance of the opportunistic BS-selection scheme significantly degrades compared to the other schemes. For large backhaul capacity, the wind-spinner clustering scheme outperforms the others at moderate powers. The scheme proposed in this paper outperforms all other schemes for sufficiently large powers,

irrespectively of the available backhaul capacity. From Figure 8d we observe that under strong interference, $\alpha = 0.5$, the proposed scheme outperforms all other schemes at all power levels even when backhaul capacity is moderate and even when only two cooperation rounds are permitted.

V. Concluding Remarks

The paper presents upper and lower bounds on the DoF of the uplink of a sectorized cellular network with backhaul cooperation between BSs. A main feature of this paper is that this DoF is characterized as a function of the backhaul rate and *the maximum number of allowed cooperation rounds*. The presented results show that limiting the number of cooperation rounds also limits the DoF achievable over the network. In particular, by Theorem 2, if the number of transmit antennas in a sector equals the number of its receive antennas $KL = M$, then to get a per-sector DoF of M, an infinite number of cooperation rounds is required as the number of cells in the network grows. If the number of cooperation rounds does not grow with the number of the cells but is bounded, then also the DoF is bounded away from M, even in the idealized case of unlimited backhaul cooperation capacity.

The upper bound on the DoF is information-theoretic and applies to *any* coding scheme. The lower bound is based on a practically implementable scheme: the transmitting mobiles either remain silent or use Gaussian point-to-point codes; receiving BSs apply vector quantizers to their M-dimensional receive signals and send the quantization messages over the backhaul links to so called master BSs which decode a cluster of messages based on its own receive signals and the quantization signals it receives over the backhaul links. No advanced tools such as interference alignment are required in this scheme. The main novelty of the scheme is the proposed choice of which mobiles remain silent and which transmit their messages. In fact, this choice exploits the sectorization of the network and is done in such a way that only few users remain silent but the network still decomposes into non-interfering clusters. The decomposition ensures that interference is not propagated across clusters and therefore facilitates decoding at the BSs.

The scheme is shown to attain not only an improved DoF, but also improved average per-user rate in the finite SNR regime.

It is straightforward to obtain the dual results for the downlink. A discussion on uplink and downlink dualities for networks with cooperation is included e.g., in [32]. To this end, BSs should first send messages to their closest master cells, which then *jointly encodes all its available messages*, i.e., it pre-calculates the transmit signals at the close-by BSs. These transmit signals are quantized and distributed over the backhaul links to their respective BSs, which in turn send these quantized signals over the network. Mobile users apply simple point-to-point reception techniques. This however does not limit their achievable DoF if the master cell has well encoded the messages, i.e., has chosen a good precoding matrix.

Appendix A
Analysis of the Uplink Scheme With Cooperative BSs

In the first subsection, we analyze the achievable DoF and required backhaul DoF of the proposed uplink scheme in Section III. In the second subsection we analyze the scheme's achievable rates and required cooperation rates at finite SNR.

A. High-SNR Analysis

Consider the scheme in Section III. As before, the quantization rate R_q is chosen as in (19). This choice allows us to achieve the same DoF as if the master BSs directly had access to all the receive signals for which they receive quantization information. Each BS in the first $\gamma - 1$ layers sends three quantization messages (one for each sector) to the master cell; three of the BSs in layer γ send no quantization information at all; and the remaining BSs in layer γ send a single quantization message. Since each layer $\ell = 1, 2, \ldots$ contains 6ℓ cells, each master BS receives in total

$$3 \cdot \sum_{\ell=1}^{\gamma-1} 6\ell + (6\gamma - 3) = 9\gamma(\gamma - 1) + 6\gamma - 3 = 3(3\gamma^2 - \gamma - 1) \tag{33}$$

quantization messages. Each such quantization message describes an M-dimensional receive signal. With these quantization messages and the 3 M-dimensional receive signals observed in its own cell, a master BS decodes the messages of $3\gamma(3\gamma-1)K$ mobile users (the $3K$ mobile users in its own cell and the $3(3\gamma^2-\gamma-1)K$ mobile users in the other active sectors of the cluster). Since each mobile user is equipped with L transmit antennas and $LK \geq M$, and since the master cell applies joint decoding like a MIMO multi-access receiver, the mobile users can reliably transmit their messages at a sum-DoF equal to $M \cdot 3\gamma(3\gamma - 1)$.

To calculate the average per-sector DoF over the entire network, we describe a cell partitioning that associates each cell to a unique master cell, and that associates the same number of cells to each master cell. The average per-user DoF is then obtained by dividing the DoF achieved at a given master cell, i.e., $M \cdot 3\gamma(3\gamma-1)$, by the total number of sectors that are contained in a single subset of the proposed cell partitioning. For $N \gg 1$ the desired cell partitioning can be obtained by associating to each master BS a set of sectors that includes *all* its layer-$1, \ldots, \gamma - 1$ cells and the layer-γ cells that lie on its north-east, east, and south-east, excluding the corner cells in the north and the south. (Recall Figure 4.)

Each subset of the described cell partitioning thus includes a master cell, all its layer-$1, 2, \ldots, \gamma - 1$ cells, and half of its layer-γ cells minus one. Its total number of cells is thus:

$$1 + \sum_{\ell=1}^{\gamma-1} 6\ell + (3\gamma - 1) = 3\gamma^2, \tag{34}$$

and it includes $3 \cdot 3\gamma^2$ sectors. We conclude that the proposed scheme achieves an average per-sector DoF of

$$\mathsf{DoF}_\gamma = \frac{M \cdot 3\gamma(3\gamma - 1)}{3 \cdot 3\gamma^2} = M\frac{3\gamma - 1}{3\gamma}, \quad \gamma \in \left\{1, \ldots, \left\lfloor \frac{\Delta}{2} \right\rfloor\right\}. \tag{35}$$

We next analyze the backhaul load that is associated with a single master cell. During Rounds $1,\ldots,\gamma$, a master BS receives a quantization message of DoF M for each of the sectors that have active users and that are closer to this master BS than to any other master BS. Since the quantization message for a sector in layer-ℓ is communicated over ℓ backhaul links, the total backhaul DoF on these rounds is

$$3M\sum_{\ell=1}^{\gamma-1} 6\ell\cdot\ell + M(6\gamma-3)\gamma = 3M\gamma^2(2\gamma-1). \quad (36)$$

Because all messages are assumed to have the same rate, during Rounds $\gamma+1,\ldots,2\gamma$ a set of decoded messages corresponding to DoF M is communicated from the master BS to the BSs for each quantization message that has been sent during Rounds $1,\ldots,\gamma$. Therefore, the total backhaul load during Rounds $1,\ldots\gamma$ coincides with the total backhaul load during Rounds $\gamma+1,\ldots,2\gamma$, and the total backhaul load over all rounds is

$$6M\gamma^2(2\gamma-1). \quad (37)$$

To balance the backhaul load and to achieve fairness among the rates achieved by the various mobile users, instances of the presented scheme are time-shared, where in different instances different cells play the role of the master cells and different routing options are used for the cooperation messages. Under such a time-sharing framework, the *average backhaul DoF* is the limiting quantity. Consider again the cell partitioning proposed above to calculate the DoF. The average backhaul DoF is obtained by dividing (37) by the number of outgoing (or incoming) backhaul links pertaining to a single subset of the cell partitioning, which by (34) is $6\cdot 3\gamma^2$:

$$\mu_{\text{DoF},\gamma} = \frac{2\cdot 3M\gamma^2(2\gamma-1)}{6\cdot 3\gamma^2} = M\frac{2\gamma-1}{3}, \qquad \gamma\in\left\{1,\ldots,\left\lfloor\frac{\Delta}{2}\right\rfloor\right\}. \quad (38)$$

B. Finite SNR Analysis

We now analyze the scheme of Section III at finite SNR, where for simplicity we restrict to single transmit and receive antennas, $M=L=1$, and to a single user per sector, $K=1$. For a given parameter γ, we choose the quantization rate as

$$R_q := \frac{3}{2\gamma-1}\mu. \quad (39)$$

By similar arguments to (38), this choice ensures that the backhaul rate-limitation (8) is satisfied. We assume that the BSs adjust their quantizers to the channel realization. Then, if $\mathbf{h}_u$ denotes the channel vector from all the users to the single receive antenna in sector u, the rate chosen above implies that the quantized signal in this sector u has a quantization noise variance of:

$$\sigma_{q,u}^2 = \frac{P\|\mathbf{h}_u\|^2+1}{2^{2R_q}-1} = \frac{P\|\mathbf{h}_u\|^2+1}{2^{\frac{6}{2\gamma-1}\mu}-1}. \quad (40)$$

Recall that the quantization noises are independent across antennas. Hence the $3\gamma(3\gamma-1)\times 3\gamma(3\gamma-1)$ (quantization and thermal) noise covariance matrix K_n for the decoding at a given master BS is given by:

$$\mathsf{K}_n := \Sigma_{q,\gamma} + \mathsf{I}, \quad (41)$$

where I denotes the identity matrix and $\Sigma_{q,\gamma}$ the diagonal matrix with 0 in the diagonal entry corresponding to the sectors of the master cells and $\sigma_{q,u}^2$ in the diagonal entry corresponding to any other given sector u of the cluster. By standard multi-access results, the maximum achievable sum-rate in a cluster is then equal to

$$R_{\text{sum}} = \frac{1}{2}\cdot\log\frac{|P\mathsf{H}_\gamma\mathsf{H}_\gamma^{\mathsf{T}}+\mathsf{K}_n|}{|\mathsf{K}_n|}. \quad (42)$$

To calculate the average per-user achievable rate, we consider again the cell-partitioning described as in Figure 4, where a set of $3\gamma^2$ cells is associated with each master cell. The average per-user (or per-sector) achievable rate is then obtained by dividing (42) by $3\cdot 3\gamma^2$.

APPENDIX B
PROOF OF THEOREM 2

The proof idea of our upper bounds is similar to [29, Lemma 1]. While [29, Lemma 1] is for Wyner's linear soft-handoff model, here we prove a similar result for the hexagonal model. Technically, the main novelty is in identifying appropriate cell partitionings based on which the genie information will be defined.

We assume that $M=KL$, and shall prove

$$\mathsf{DoF}\left(\mu_{\text{DoF}},\Delta\right) \le M\cdot\left(\frac{1}{2}+\frac{2}{3}\mu_{\text{DoF}}\right). \quad (43)$$

The proof of the other upper bound uses a similar method and is omitted. To prove (43), partition the cells of the network alternately into red and white cells as depicted in Figure 9. Then, define

$$\begin{aligned}
\mathbb{W}_{\text{red}} &:= \{W_u^{(k)}\colon u \text{ is in a red cell and } k=1,\ldots,K\}\\
\mathbb{X}_{\text{red}} &:= \{\mathbf{X}_u^{(k)}\colon u \text{ is in a red cell and } k=1,\ldots,K\}\\
\mathbb{Y}_{\text{red}} &:= \{\mathbb{Y}_i\colon i \text{ is a red cell}\}\\
\mathbb{Y}_{\text{white}} &:= \{\mathbb{Y}_i\colon i \text{ is a white cell}\}\\
\mathbb{Z}_{\text{red}} &:= \{\mathbb{Z}_i\colon i \text{ is a red cell}\}\\
\mathbb{Z}_{\text{white}} &:= \{\mathbb{Z}_i\colon i \text{ is a white cell}\}
\end{aligned}$$

as well as for each round $d=1,\ldots,\Delta$, the conferencing messages

$$\mathbb{V}_{\text{white}\to\text{red}}^{(d)} := \left\{V_{i\to j}^{(d)}\colon i \text{ is a white cell},\ j \text{ is a red cell}\right\}, \quad (44)$$

and $\mathbb{V}_{\text{red}\to\text{red}}^{(d)}$, $\mathbb{V}_{\text{red}\to\text{white}}^{(d)}$, and $\mathbb{V}_{\text{white}\to\text{white}}^{(d)}$, which are defined similarly.

To prove the converse, for each blocklength n fix encoding, cooperation, and decoding functions $\{f_u^{(k)}\}$, $\{\psi_{j,i}^{(d)}\}$, and $\{h_j\}$ so that for sufficiently large blocklength n the probability of error does not exceed $\epsilon>0$. We show in the following that a super-receiver observing the three items listed in the following can decode all transmitted messages $\{W_u^{(k)}\colon u=$

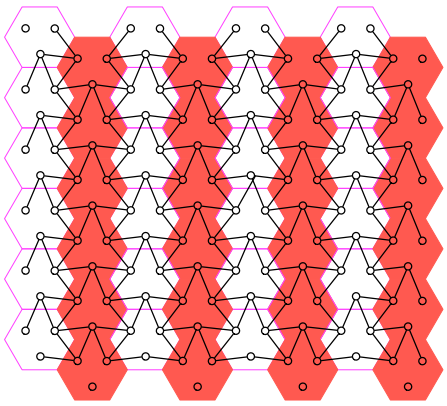

Fig. 9. Cell partitioning used for the first converse bound.

$1,\ldots,3N,\ k=1,\ldots,K\}$ correctly whenever the N BSs decode them correctly in the original setup. The super-receiver's probability of error thus cannot be larger than the original probability of error, which was upper-bounded by ϵ. The three items are:

1) all output signals in red cells, $\mathbb{Y}_{\text{red}}$;
2) all conferencing messages from white to red cells, $\mathbb{V}^1_{\text{white}\to\text{red}},\ldots,\mathbb{V}^{\Delta}_{\text{white}\to\text{red}}$; and
3) the genie-information

$$\mathbb{G} := \tilde{\mathsf{H}}_{\text{white}\to\text{white}}\tilde{\mathsf{H}}^{-1}_{\text{white}\to\text{red}}\mathbb{Z}_{\text{red}} - \mathbb{Z}_{\text{white}}, \tag{45}$$

where for each pair of colours $c,c' \in \{\text{red, white}\}$ we denote by $\tilde{\mathsf{H}}_{c,c'}$ the channel matrix from mobile users in cells of colour c to BSs in cells of colour c'. In particular, we impose that the diagonal entries of the matrix $\tilde{\mathsf{H}}_{\text{white}\to\text{red}}$ measure the channel coefficients from mobile users in a sector of a white cell to the BS of an adjacent interfering sector in a red cell. (It is easy to check that $\tilde{\mathsf{H}}_{\text{white}\to\text{red}}$ is invertible with probability 1, so the genie-information in (45) is well-defined.)

The super-receiver decodes the messages $\{W_u^{(k)}\}$ by means of the following six decoding steps:

1) For each round $d=1,\ldots,\Delta$, it applies the appropriate cooperation functions $\{\psi^{(d)}_{j,i}\}$ to the red output signals $\mathbb{Y}_{\text{red}}$ and the previous rounds' conferencing messages $\{\mathbb{V}^{(d')}_{\text{white}\to\text{red}}\}^{d-1}_{d'=1}$ and $\{\mathbb{V}^{(d')}_{\text{red}\to\text{red}}\}^{d-1}_{d'=1}$. This allows the super-receiver to compute the conferencing messages of the current round $\mathbb{V}^{(d)}_{\text{red}\to\text{red}}$. (Notice that knowledge of output signals in white cells or conferencing messages sent *to* white cells are not required for this computation.)
2) It applies the appropriate decoding functions $\{h_j\colon j \text{ is a red cell}\}$ to the output signals $\mathbb{Y}_{\text{red}}$ and the conferencing messages $\{\mathbb{V}^{(d)}_{\text{red}\to\text{red}}\}^{\Delta}_{d=1}$ to decode messages $\mathbb{W}_{\text{red}}$.
3) It applies the encoding functions $\{f_u^{(k)}\}$ to the previously decoded messages $\mathbb{W}_{\text{red}}$ to construct input signals $\mathbb{X}_{\text{red}}$.
4) With the input and output signals sent and received in red cells, $\mathbb{X}_{\text{red}}$ and $\mathbb{Y}_{\text{red}}$, it reconstructs the output signals received at the BSs in the white cells by forming:

$$\mathbb{Y}_{\text{white}} = \tilde{\mathsf{H}}_{\text{white}\to\text{white}}\tilde{\mathsf{H}}^{-1}_{\text{white}\to\text{red}}(\mathbb{Y}_{\text{red}} - \tilde{\mathsf{H}}_{\text{red}\to\text{red}}\mathbb{X}_{\text{red}}) + \tilde{\mathsf{H}}_{\text{red}\to\text{white}}\mathbb{X}_{\text{red}} - \mathbb{G}. \tag{46}$$

5) For each round $d=1,\ldots,\Delta$, it applies the appropriate cooperation functions $\{\psi^{(d)}_{j,i}\}$ to the white and red output signals $\mathbb{Y}_{\text{white}}$ and $\mathbb{Y}_{\text{red}}$ and to the observed and previously calculated conferencing messages $\{\mathbb{V}^{(d')}_{\text{white}\to\text{red}}\}^{d-1}_{d'=1}$ and $\{\mathbb{V}^{(d')}_{\text{red}\to\text{white}}\}^{d-1}_{d'=1}$, $\{\mathbb{V}^{(d')}_{\text{red}\to\text{red}}\}^{d-1}_{d'=1}$, $\{\mathbb{V}^{(d')}_{\text{white}\to\text{white}}\}^{d-1}_{d'=1}$, to compute the conferencing messages of the current round $\mathbb{V}^{(d)}_{\text{red}\to\text{white}}$ and $\mathbb{V}^{(d)}_{\text{white}\to\text{white}}$.
6) It applies the appropriate decoding functions $\{h_j\colon j \text{ is a white cell}\}$ to the output signals $\mathbb{Y}_{\text{white}}$ and the calculated conferencing messages $\{\mathbb{V}^{(d)}_{\text{red}\to\text{white}}\}^{\Delta}_{d=1}$ and $\{\mathbb{V}^{(d)}_{\text{white}\to\text{white}}\}^{\Delta}_{d=1}$ so as to decode messages $\mathbb{W}_{\text{white}}$.

The above arguments imply that any $3NK$-tuple $(R_1^{(1)},\ldots,R_{3N}^{(K)})$ that is achievable over the original network from mobile users to BSs is also achievable over the network from mobile users to the super-receiver. So, by Fano's inequality:

$$\begin{aligned}
&\sum_{u=1}^{3N}\sum_{k=1}^{K} R_u^{(k)} - \epsilon \\
&\le \frac{1}{n} I\big(W_1^{(1)},\ldots,W_{3N}^{(K)};\mathbb{Y}_{\text{red}},\mathbb{V}^1_{\text{white}\to\text{red}},\ldots,\mathbb{V}^{\Delta}_{\text{white}\to\text{red}},\mathbb{G}\big) \\
&= \frac{1}{n} I\big(W_1^{(1)},\ldots,W_{3N}^{(K)};\mathbb{Y}_{\text{red}}\big) \\
&\quad + \frac{1}{n} I\big(W_1^{(1)},\ldots,W_{3N}^{(K)};\mathbb{V}^1_{\text{white}\to\text{red}}\cdots,\mathbb{V}^{\Delta}_{\text{white}\to\text{red}}\big|\mathbb{G},\mathbb{Y}_{\text{red}}\big) \\
&\quad + \frac{1}{n} I\big(W_1^{(1)},\ldots,W_{3N}^{(K)};\mathbb{G}\big|\mathbb{Y}_{\text{red}}\big),
\end{aligned} \tag{47}$$

where ϵ tends to zero as $n\to\infty$. We notice that the first summand in (47) has DoF at most 3 $M|\mathcal{I}_{\text{red}}|$, where $\mathcal{I}_{\text{red}} := \{i\colon \text{cell } i \text{ is red}\}$; the second summand in (47) has DoF at most $4|\mathcal{I}_{\text{white}}|\cdot\mu_{\mathsf{DoF}}$, where $\mathcal{I}_{\text{white}} := \{i\colon \text{cell } i \text{ is white}\}$; and the third summand in (47) has zero DoF because, for any N:

$$\begin{aligned}
I(W_1^{(1)},\ldots,W_{3N}^{(K)};\mathbb{G}|\mathbb{Y}_{\text{red}}) &\le h(\mathbb{G}) - h(\mathbb{G}|\mathbb{Z}_{\text{red}}) &(48)\\
&= h(\mathbb{G}) - h(\mathbb{Z}_{\text{white}}), &(49)
\end{aligned}$$

which is finite and does not grow with power P, irrespectively of the chosen encoding, cooperation, and decoding functions. Dividing (47) by $1/2\log(1+P)$ and taking the limit $P\to\infty$, we obtain the following bound on the DoF:

$$3\ N\cdot\mathsf{DoF} \le 3\ M|\mathcal{I}_{\text{red}}| + 4|\mathcal{I}_{\text{white}}|\cdot\mu_{\mathsf{DoF}}. \tag{50}$$

Dividing the above by 3 N and letting $N\to\infty$ establishes the desired bound after noticing that

$$\overline{\lim_{N\to\infty}}\frac{|\mathcal{I}_{\text{red}}|}{N} = \overline{\lim_{N\to\infty}}\frac{|\mathcal{I}_{\text{white}}|}{N} = 1/2. \tag{51}$$

ACKNOWLEDGMENT

The authors thank P. Ciblat for helpful discussions.

REFERENCES

[1] S. Gelincik, M. Wigger, and L. Wang, "DoF in sectored cellular systems with BS cooperation under a complexity constraint," in *Proc. 15th Int. Symp. Wireless Commun. Syst. (ISWCS)*, Lisbon, Portugal, Aug. 2018, pp. 1–5.

[2] R. Nasri and A. Jaziri, "Analytical tractability of hexagonal network model with random user location," *IEEE Trans. Wireless Commun.*, vol. 15, no. 5, pp. 3768–3780, May 2016.

[3] T. T. Tesfay, R. Khalili, J.-Y. Le Boudec, F. Richter, and A. Fehske, "Energy saving and capacity gain of micro sites in regular LTE networks: Downlink traffic layer analysis," in *Proc. 6th ACM workshop Perform. Monit. Meas. Heterogeneous Wireless Wired Netw. (PM2HWN)*, 2011, pp. 83–92.

[4] M. Bacha, J. Evans, and S. Hanly, "On the capacity of cellular networks with MIMO links," in *Proc. IEEE Int. Conf. Commun.*, Jun. 2006, pp. 1337–1342.

[5] V. Ntranos, M. A. Maddah-Ali, and G. Caire, "Cellular interference alignment," *IEEE Trans. Inf. Theory*, vol. 61, no. 3, pp. 1194–1217, Mar. 2015.

[6] M. Bande, A. El Gamal, and V. V. Veeravalli, "Degrees of freedom in wireless interference networks with cooperative transmission and backhaul load constraints," *IEEE Trans. Inf. Theory*, vol. 65, no. 9, pp. 5816–5832, Sep. 2019.

[7] S. A. Jafar, "Interference alignment: A new look at signal dimensions in a communication network," *Found. Trends Commun. Inf. Theory*, vol. 7, no. 1, pp. 1–134, 2011.

[8] G. Sridharan and W. Yu, "Degrees of freedom of MIMO cellular networks: Decomposition and linear beamforming design," *IEEE Trans. Inf. Theory*, vol. 61, no. 6, pp. 3339–3364, Jun. 2015.

[9] A. Sanderovich, S. Shamai, Y. Steinberg, and G. Kramer, "Communication via decentralized processing," *IEEE Trans. Inf. Theory*, vol. 54, no. 7, pp. 3008–3023, Jul. 2008.

[10] D. Gesbert, S. Hanly, H. Huang, S. Shamai Shitz, O. Simeone, and W. Yu, "Multi-cell MIMO cooperative networks: A new look at interference," *IEEE J. Sel. Areas Commun.*, vol. 28, no. 9, pp. 1380–1408, Dec. 2010.

[11] S.-N. Hong and G. Caire, "Compute-and-forward strategies for cooperative distributed antenna systems," *IEEE Trans. Inf. Theory*, vol. 59, no. 9, pp. 5227–5243, Sep. 2013.

[12] China Mobile Research Institute. (Oct. 2011). *C-RAN: The Road Towards Green RAN*. [Online]. Available: https://labs.chinamobile.com/cran

[13] M. Peng, C. Wang, V. Lau, and H. V. Poor, "Fronthaul-constrained cloud radio access networks: Insights and challenges," *IEEE Wireless Commun.*, vol. 22, no. 2, pp. 152–160, Apr. 2015.

[14] L. Zhou and W. Yu, "Uplink multicell processing with limited backhaul via Per-Base-Station successive interference cancellation," *IEEE J. Sel. Areas Commun.*, vol. 31, no. 10, pp. 1981–1993, Oct. 2013.

[15] O. Simeone, A. Maeder, M. Peng, O. Sahin, and W. Yu, "Cloud radio access network: Virtualizing wireless access for dense heterogeneous systems," *J. Commun. Netw.*, vol. 18, no. 2, pp. 135–149, Apr. 2016.

[16] M. Peng, Y. Sun, X. Li, Z. Mao, and C. Wang, "Recent advances in cloud radio access networks: System architectures, key techniques, and open issues," *IEEE Commun. Surveys Tuts.*, vol. 18, no. 3, pp. 2282–2308, 3rd Quart., 2016.

[17] I. Estella Aguerri, A. Zaidi, G. Caire, and S. Shamai (Shitz), "On the capacity of cloud radio access networks with oblivious relaying," *IEEE Trans. Inf. Theory*, vol. 65, no. 7, pp. 4575–4596, Jul. 2019.

[18] S. Gelincik and G. Rekaya-Ben Othman, "Degrees-of-freedom in multi-cloud based sectored cellular networks," *Entropy*, vol. 22, no. 6, p. 668, Jun. 2020.

[19] M. Singhal, T. Seyfi, and A. El Gamal, "Joint uplink-downlink cooperative interference management with flexible cell associations," *IEEE Trans. Commun.*, vol. 68, no. 9, pp. 5420–5434, Sep. 2020.

[20] F. Willems, "The discrete memoryless multiple access channel with partially cooperating encoders (Corresp.)," *IEEE Trans. Inf. Theory*, vol. 29, no. 3, pp. 441–445, May 1983.

[21] A. Sendonaris, E. Erkip, and B. Aazhang, "User cooperation diversity—Part I: System description," *IEEE Trans. Commun.*, vol. 51, no. 11, pp. 1927–1938, Nov. 2003.

[22] A. Sendonaris, E. Erkip, and B. Aazhang, "User cooperation diversity—Part II: Implementation aspects and performance analysis," *IEEE Trans. Commun.*, vol. 51, no. 11, pp. 1939–1948, Nov. 2003.

[23] G. Kramer, I. Marić, and R. D. Yates, "Cooperative communications," *Found. Trends Netw.*, vol. 1, nos. 3–4, pp. 271–425, 2007.

[24] S. I. Bross, A. Lapidoth, and M. A. Wigger, "The Gaussian MAC with conferencing encoders," in *Proc. IEEE Int. Symp. Inf. Theory*, Jul. 2008, pp. 2702–2706.

[25] M. A. Wigger and G. Kramer, "Three-user MIMO MACs with cooperation," in *Proc. IEEE Inf. Theory Workshop Netw. Inf. Theory*, Jun. 2009, pp. 221–225.

[26] E. Aktas, J. Evans, and S. Hanly, "Distributed decoding in a cellular multiple-access channel," *IEEE Trans. Wireless Commun.*, vol. 7, no. 1, pp. 241–250, Jan. 2008.

[27] M. N. Bacha, J. S. Evans, and S. V. Hanly, "On the capacity of MIMO cellular networks with macrodiversity," in *Proc. Austral. Commun. Theory Workshop*, Perth, WA, Australia, Feb. 2006, pp. 105–109.

[28] O. Simeone, O. Somekh, H. V. Poor, and S. Shamai, "Local base station cooperation via finite-capacity links for the uplink of linear cellular networks," *IEEE Trans. Inf. Theory*, vol. 55, no. 1, pp. 190–204, Jan. 2009.

[29] M. Wigger, R. Timo, and S. Shamai (Shitz), "Conferencing in Wyner's asymmetric interference network: Effect of number of rounds," *IEEE Trans. Inf. Theory*, vol. 63, no. 2, pp. 1199–1226, Feb. 2017.

[30] O. Simeone *et al.*, "Cooperative wireless cellular systems: An information-theoretic view," *Found. Trends Commun. Inf. Theory*, vol. 8, nos. 1–2, pp. 1–177, 2012.

[31] A. Sanderovich, O. Somekh, H. V. Poor, and S. Shamai (Shitz), "Uplink macro diversity of limited backhaul cellular network," *IEEE Trans. Inf. Theory*, vol. 55, no. 8, pp. 3457–3478, Aug. 2009.

[32] V. V. Veeravalli and A. El Gamal, *Interference Management in Wireless Networks: Fundamental Bounds and the Role of Cooperation*. Cambridge, U.K.: Cambridge Univ. Press, 2018.

[33] W. Yu, T. Kwon, and C. Shin, "Multicell coordination via joint scheduling, beamforming, and power spectrum adaptation," *IEEE Trans. Wireless Commun.*, vol. 12, no. 7, pp. 1–14, Jul. 2013.

[34] E. Atsan, R. Knopp, S. Diggavi, and C. Fragouli, "Towards integrating quantize-map-forward relaying into LTE," in *Proc. IEEE Inf. Theory Workshop*, Sep. 2012, pp. 212–216.

[35] M. N. Khormuji and E. G. Larsson, "Improving collaborative transmit diversity by using constellation rearrangement," in *Proc. IEEE Wireless Commun. Netw. Conf.*, Mar. 2007, pp. 803–807.

[36] J. N. Laneman, G. W. Wornell, and D. N. C. Tse, "An efficient protocol for realizing cooperative diversity in wireless networks," in *Proc. IEEE Int. Symp. Inf. Theory*, Jun. 2001, p. 294.

[37] J. Chen, U. Mitra, and D. Gesbert, "Optimal UAV relay placement for single user capacity maximization over terrain with obstacles," in *Proc. IEEE 20th Int. Workshop Signal Process. Adv. Wireless Commun. (SPAWC)*, Jul. 2019, pp. 1–5.

[38] S.-J. Kim, S. Jain, and G. B. Giannakis, "Backhaul-constrained multi-cell cooperation using compressive sensing and spectral clustering," in *Proc. IEEE 13th Int. Workshop Signal Process. Adv. Wireless Commun. (SPAWC)*, Cesme, Turkey, Jun. 2012, pp. 65–69.

[39] G. Katz, B. M. Zaidel, and S. S. Shitz, "On layered transmission in clustered cooperative cellular architectures," in *Proc. IEEE Int. Symp. Inf. Theory*, Istanbul, Turkey, Jul. 2013, pp. 1162–1166.

[40] N. Levy and S. Shamai, "Clustered local decoding for Wyner-type cellular models," *IEEE Trans. Inf. Theory*, vol. 55, no. 11, pp. 4967–4985, Nov. 2009.

[41] W. Rhee and J. M. Cioffi, "On the capacity of multiuser wireless channels with multiple antennas," *IEEE Trans. Inf. Theory*, vol. 49, no. 10, pp. 2580–2595, Oct. 2003.

[42] A. D. Wyner, "Shannon-theoretic approach to a Gaussian cellular multiple-access channel," *IEEE Trans. Inf. Theory*, vol. 40, no. 6, pp. 1713–1727, Nov. 1994.

[43] S. Shamai (Shitz) and A. D. Wyner, "Information-theoretic considerations for symmetric, cellular, multiple-access fading channels. I," *IEEE Trans. Inf. Theory*, vol. 43, no. 6, pp. 1877–1894, Nov. 1997.

[44] E. Aktas, J. Evans, and S. Hanly, "Distributed decoding in a cellular multiple-access channel," in *Proc. Int. Symp. Inf. Theory (ISIT)*, 2004, p. 484.

[45] T. M. Cover and J. A. Thomas, *Elements of Information Theory* (Wiley Series in Telecommunications and Signal Processing). Hoboken, NJ, USA: Wiley, 2006.

[46] A. El Gamal and V. V. Veeravalli, "Flexible backhaul design and degrees of freedom for linear interference networks," in *Proc. IEEE Int. Symp. Inf. Theory*, Jun. 2014, pp. 2694–2698.

[47] S. Gelincik, L. Wang, and M. Wigger, "Cell sector-clustering for joint decoding of messages," Application Patent PCT/EP2018/059 535, Apr. 13, 2018.

Samet Gelincik (Member, IEEE) received the B.Sc. degree in electrical and electronics engineering from Hacettepe University, Ankara, Turkey, in 2010, the M.Sc. degree in electrical and electronics engineering from Middle East Technical University (METU), Ankara, in 2014, and the Ph.D. degree from the Institute Polytechnique de Paris, Telecom Paris, France, in 2019. He is currently a Post-Doctoral Researcher with IETR, INSA de Rennes, France. His research interests include the fields of communication and information theory and error correcting codes with the emphasis on polar codes.

Michèle Wigger (Senior Member, IEEE) received the M.Sc. degree (Hons.) in electrical engineering and the Ph.D. degree in electrical engineering from ETH Zürich in 2003 and 2008, respectively. In 2009, she was first a Post-Doctoral Fellow with the University of California at San Diego, San Diego, USA, and then joined Telecom Paris, France, where she is currently a Full Professor. She has held visiting professor appointments at the Technion–Israel Institute of Technology and ETH Zürich. Her research interest includes multiterminal information theory, in particular in distributed source coding and in capacities of networks with states, feedback, user cooperation, or caching. She has served as an Associate Editor for the IEEE COMMUNICATION LETTERS and for Shannon Theory for the IEEE TRANSACTIONS ON INFORMATION THEORY. From 2016 to 2019, she also served on the Board of Governors of the IEEE Information Theory Society.

Ligong Wang (Member, IEEE) received the B.E. degree in electronic engineering from Tsinghua University, Beijing, China, in 2004, and the M.Sc. and Dr.Sc. degrees in electrical engineering from ETH Zürich, Switzerland, in 2006 and 2011, respectively. From 2011 to 2014, he was a Post-Doctoral Associate with the Department of Electrical Engineering and Computer Science, Massachusetts Institute of Technology, Cambridge, MA, USA. He is currently a Researcher (chargé de recherche) with CNRS, France, and the ETIS Laboratory, Cergy-Pontoise. His research interests include classical and quantum information theory, physical-layer security, and digital, in particular optical communications. Since 2019, he has been serving as an Associate Editor for Shannon Theory for the IEEE TRANSACTIONS ON INFORMATION THEORY.